Integration of radiative transfer into satellite models of ocean primary production

T. J. Smyth, G. H. Tilstone, and S. B. Groom
Remote Sensing Group, Plymouth Marine Laboratory, Plymouth, UK

Received 22 October 2004; revised 4 May 2005; accepted 5 July 2005; published 14 October 2005.

[1] A major goal of ocean color observations from space is the determination of phytoplankton primary productivity (PP) and hence oceanic carbon uptake. Results of a PP model implemented to use satellite-derived fields of chlorophyll, photosynthetically available radiation (PAR) and sea-surface temperature (SST) are presented. The model gave a global estimate of PP of around 57 Gt C yr^{-1} and gives a low RMS (0.16) when compared with in situ data. However, as the model's in-water light field parameterization only considers attenuation by pure water and chlorophyll, PP is overestimated in case II waters where other optically important constituents such as colored dissolved organic matter (CDOM) and suspended particulate matter (SPM) are also present. This paper develops a novel technique to determine PP by coupling a radiative transfer code, which allows the inclusion of CDOM and SPM, to the original photosynthesis model. For the global calculations, a look-up table has been generated using chlorophyll, CDOM, SST, PAR and day length as inputs. The resultant 364,500 element look-up table has been applied to data from the Sea-viewing Wide Field-of-view Sensor (SeaWiFS) and Moderate-Resolution Imaging Spectroradiometer (MODIS). PP retrievals are improved in case II waters and global estimates are reduced to between 52 and 55 Gt C yr^{-1}.

Citation: Smyth, T. J., G. H. Tilstone, and S. B. Groom (2005), Integration of radiative transfer into satellite models of ocean primary production, *J. Geophys. Res.*, *110*, C10014, doi:10.1029/2004JC002784.

1. Introduction

[2] Primary productivity (PP) is the amount of carbon fixed by plants over time through photosynthesis and forms a fundamental basis for both the terrestrial and marine food webs. Current estimates place the amount of carbon fixed by phytoplankton to be between 45 and 50 Gt C yr^{-1} accounting for 48% of the total global carbon uptake [*Field et al.*, 1998]. PP therefore represents a key process for the (oceanic) carbon cycle [*Antoine et al.*, 1996] and global observations and modeling are required to further improve these estimates.

[3] Determining global totals of marine PP using in situ radiocarbon [*Joint and Pomroy*, 1986], oxygen [*Williams et al.*, 1979] or Fast Repetition Rate Fluorometry [*Kolber and Falkowski*, 1993] measurements is an impossible task because of cost, data sparsity and bias issues: Research cruises tend to last less than a month; they tend to sample "unique" or interesting events; and generally occur during the more clement months of the year. Therefore if global and regional totals of PP are to be determined, satellite data must be used.

[4] Several models, using a variety of approaches, exist to determine PP using satellite data. An excellent review and classification of PP models in general can be found in [*Behrenfeld and Falkowski*, 1997b]; comparisons have also been made between the various formulations as part of the Third Primary Production Algorithm Round-Robin (PPARR3 [*Carr et al.*, 2005]). Generally the PP models they describe have been parameterized using data from case I waters, i.e., where variations in the ocean color are determined by phytoplankton and their covarying biological by-products. In case II waters the optical signal is complicated by the addition of other substances that vary independently of phytoplankton such as Colored Dissolved Organic Matter (CDOM) and Suspended Particulate Matter (SPM). Case II waters tend to be in coastal areas (although not all coastal waters can be described as case II) where riverine input and sediment resuspension play a significant role in determining the optical characteristics. Chlorophyll retrievals by satellite in case II waters are often hampered by the presence of CDOM and SPM, which cause the in-water light field to be altered, causing inaccuracies in the estimation of PP. Current estimates of coastal zone PP infer that these regions account for 30% of global ocean production despite only accounting for 10% of the global ocean surface area [*Wollast*, 1998].

[5] Photosynthesis, being a light-driven process, is best described using accurate spectral models of light attenuation. These improvements are primarily realized in the deeper depths of the water column where photosynthesis is actually light-limited (as opposed to near the surface where photosynthesis is light-saturated and thus less dependent on an accurate description of the light field) and in determining the depth at which the transition occurs be-

0148-0227/05/2004JC002784

tween light-limited (α) and light-saturated (P_{max}) photosynthesis (i.e., the depth corresponding to the light saturation parameter, $E_k = P_{max}/\alpha$). Estimates of PP using a nonspectral approach may be overestimated by as much as 50% or more [*Platt and Sathyendranath*, 1991].

[6] [*Liu et al.*, 1999] showed that, when compared with in situ data, the spectral light model of [*Morel*, 1988] overestimated the scalar irradiance within the water column when a chlorophyll profile was used as input: An order of magnitude difference was noted in some cases. However, when a radiative transfer equation (RTE) was used the modeled and measured scalar irradiance fields gave close agreement. In this paper an RTE is coupled to the wavelength-resolved PP model of [*Morel*, 1991] in place of the spectral model of light attenuation described by *Morel* [1988]. The approach is further extended to optically complex case II waters by allowing the input of CDOM and SPM into the RTE calculations. This model is then reduced to a look-up table to allow the rapid calculation of PP and applied to global satellite fields.

[7] Research over the past 10 years has concluded that PP model performance is a function of the choice of physiological model [*Campbell et al.*, 2002] rather than model complexity (which is largely a result of spectral in-water light modeling). However, once the physiological component is well constrained, the additional benefits of advanced descriptions of the underwater light field will emerge. This paper aims to ensure that studies on physiology are paralleled by advances in the treatment of light attenuations, such that all aspects of productivity modeling develop in unison.

2. Methods

[8] The basis of the photosynthesis model is the spectral formulation of *Morel* [1991] following the parameterizations of *Morel et al.* [1996]; this can be represented using the triple integral,

$$P = 12 \int_0^L \int_0^D \int_{\lambda_2}^{\lambda_1} Chl(Z) PAR(\lambda, Z, t) \cdot a^*(\lambda) \phi_\mu(\lambda, Z, t) d\lambda dZ dt, \quad (1)$$

where P (mgC $m^{-2}d^{-1}$) is the daily realized column production, D (m) the depth of the euphotic zone (1% light level) and L (s) the day length. PAR (μ mol quanta $m^{-2}s^{-1}$) is the photosynthetically available radiation and is the integral of the spectral light field (as a function of depth) between 400 (λ_1) and 700 nm (λ_2). Chl (mg m^{-3}) is the chlorophyll concentration and a*(λ) is the absorption cross section per unit of chlorophyll pertinent to the actual spectral light field composition (m^{-1}). Finally ϕ_μ is the net growth rate expressed in terms of mol C (mol quanta)$^{-1}$; this is parameterized, following *Morel* [1991], as a function of a dimensionless parameter, x,

$$x = PUR/KPUR, \quad (2)$$

where PUR is the Photosynthetically Useful Radiation (PAR weighted by the chlorophyll-a specific absorption spectrum) and a normalizing value, KPUR, which is determined from the temperature (T),

$$KPUR(T) = KPUR(20^\circ) 1.065^{(T-20^\circ)}, \quad (3)$$

where KPUR(20°) is set to 80 μmol quanta $m^{-2}s^{-1}$ following *Morel et al.* [1996]. Here ϕ_μ is then parameterized as

$$\phi_\mu(x) = \phi_{\mu\,max} f(x), \quad (4)$$

where $\phi_{\mu max}$ is set to 0.06 mol C (mol quanta)$^{-1}$ and f(x) is formulated according to the parameters of the photosynthesis-irradiance curve following *Platt et al.* [1980],

$$f(x) = x^{-1}(1 - e^{-x})e^{-\beta x}, \quad (5)$$

where β is the (unitless) photoinhibition parameter and is set to 0.01. The satellite or in situ derived parameters of Chl and PAR (once spectrally resolved) can be put into equation (1) and the SST used within the physiological parameterizations of equations (2)–(5).

2.1. Single Station Mode

[9] The photosynthesis model can be run in single station mode using vertical profiles of chlorophyll and temperature. Measurements of the surface downwelling spectral irradiance, $E_d(\lambda)$ ($Wm^{-2}nm^{-1}$), are also required to force the model. These values can either be modeled or measured.

[10] To model $E_d(\lambda)$ the approach of *Gregg and Carder* [1990] modified to include the effects of clouds [*Reed*, 1977] was used with inputs of position, date and standard meteorological parameters (from, e.g., the European Centre for Medium-Range Weather Forecasting).

[11] $E_d(\lambda)$ is rarely continuously measured during research cruises: The measurements are generally broadband PAR with values being taken every minute or integrated over an entire day. To satisfy equation (1) these PAR values need to be time and wavelength resolved. Daily integrated PAR can be resolved into hourly PAR using the formula [*Kirk*, 2000]

$$PAR(t) = \frac{\pi PAR_{daily}}{2L} \sin\left(\frac{\pi t}{L}\right), \quad (6)$$

where L is the day length and t is time after sunrise, both in seconds.

[12] PAR(t) can then be spectrally resolved using the following approach: A look-up table (LUT) of spectral E_d values (E_dLUT), at 5 nm resolution, was generated for noon on serial day 181 at latitude 50°N using a single run of the *Gregg and Carder* [1990] model with standard meteorological parameters as input. The integrated irradiance (PAR) from this single run was found to be 1695 μmol quanta m^{-2} s^{-1}. The values of PAR(t) were then compared with this integrated value and the spectral E_d values scaled up or down accordingly. For example, if PAR(t) was 847.5 μmol quanta m^{-2} s^{-1} the entire E_d spectrum was scaled down, compared with the E_dLUT by a factor of 2. This process assumes that the only effect of clouds, changes in atmospheric

absorption and change in solar zenith angle, latitude and season are to linearly scale the spectral values of E_d.

2.1.1. Case I Formulation

[13] The light field is propagated through the water column by calculating the spectral attenuation coefficient for downwelling irradiance following the methodology of *Morel* [1991] and the tabulated values of *Morel* [1988]. This is simply formulated as

$$K(\lambda, Z) = K_w(\lambda) + K_{Chl}(Chl(\lambda, Z)), \quad (7)$$

where K_w and K_{Chl} are the pure water and chlorophyll components respectively in units of m^{-1}. However, in case II waters the optical signal is complicated by the presence of other substances and equation (7) no longer holds.

2.1.2. Case II Formulation

[14] *Liu et al.* [1999] found that when compared with a radiative transfer equation (RTE), the *Morel* [1988] modeled light field overestimates the downwelling scalar irradiance field substantially: Differences were apparent at 10 m and increased rapidly with depth with an order of magnitude deviation from in situ measurements at 60 m. This implies that values of PP will be overestimated when the photosynthesis model of equation (1) is used in conjunction with the *Morel* [1988] modeled light field.

[15] This paper builds on this finding by coupling the photosynthesis model with the RTE of *Mobley* [1995] and adding the effect of CDOM and SPM rather than simulating the profile of irradiance using just the chlorophyll profile (as in the work of *Liu et al.* [1999]). This will allow more accurate modeling of the in-water light field in optically complex case II waters and consequently, in theory at least, allow more accurate retrievals of PP in such regions. The radiative transfer code HYDROLIGHT (v3) [*Mobley*, 1995] was used and the water radiatively partitioned into three components: (1) pure water, (2) particulate matter and (3) CDOM. In terms of the Inherent Optical Properties (IOPs) the absorption can be represented thus:

$$a_t(\lambda, Z) = a_w(\lambda) + a_p(\lambda, Z) + a_{CDOM}(\lambda, Z) \qquad \left(m^{-1}\right) \quad (8)$$

$$a_p(\lambda, Z) = 0.06 A_{chl}(\lambda)(Chl(Z))^{0.65}, \quad (9)$$

where the p and w subscripts refer to the particulate and pure water [*Pope and Fry*, 1997] components, respectively, and $A_{chl}(\lambda)$ is the normalized (to 440 nm) spectral absorption values of phytoplankton pigments [*Prieur and Sathyendranath*, 1981]. The values of $a_{CDOM}(\lambda, Z)$ can be taken from in situ measurements.

[16] The scattering IOPs are described similarly,

$$b_t(\lambda, Z) = b_w(\lambda) + b_p(\lambda, Z) \qquad \left(m^{-1}\right), \quad (10)$$

$$b_p(\lambda, Z) = b_p(660, Z)(660.0/\lambda)^{\log_{10}(Chl(Z))} + b_{SPM}(\lambda, Z), \quad (11)$$

$$b_p(660, Z) = 0.407 Chl(Z)^{0.795}, \quad (12)$$

$$b_{SPM}(\lambda, Z) = (SPM(Z)/1.73)(\lambda/442.0)^{-0.4}, \quad (13)$$

where $b_w(\lambda)$ is calculated following *Morel* [1974] and equation (13) from the MERIS processing code [*Doerffer*, 2002]; SPM is the measured suspended particulate matter in units of g m^{-3}. For the scattering calculations the phase function of pure water [*Mobley*, 1994] was used for component 1 and the *Petzold* [1972] phase function was used for component 2; component 3 (CDOM) is considered to be non-scattering.

[17] The HYDROLIGHT code was run for 16 stations in the Irish Sea using measured profiles of Chl, CDOM and SPM. The effects of chlorophyll and CDOM fluorescence, bioluminescence and Raman scattering upon the spectral light field were considered to be negligible and neglected. The code was run at 5 nm resolution between 400 and 700 nm and at 1 m depth resolution. The scalar irradiance, $E_0(\lambda)$, output from HYDROLIGHT was then used to drive the photosynthesis model, i.e., coupled to equation (1).

2.2. Application to Satellite Data

2.2.1. Application to Case I

[18] For a direct application of the production model to satellite data, further simplifications and parameterizations are required. First the vertical structure of bio-physical parameters is unattainable from space using sensors such as the Sea-viewing Wide Field-of-view Sensor (SeaWiFS) and the Advanced Very High Resolution Radiometer (AVHRR) which can be used to determine chlorophyll [*O'Reilly et al.*, 1998] and sea-surface temperature (SST) [*McClain et al.*, 1985], respectively. Therefore it is assumed that the chlorophyll and temperature profiles are invariant with depth. This assumption feeds back into the parameterizations for $a^*(\lambda)$ and $\phi_\mu(\lambda, Z, t)$ which are set to the value determined from the satellite retrievals.

[19] Second, it is also useful for the model to be forced using monthly fields of chlorophyll, SST and PAR [*Frouin and Pinker*, 1995] to determine global carbon sequestration rates. The PAR monthly fields are average daily integrated values; the values of $E_d(\lambda)$ can be retrieved using the E_dLUT and the approach outlined in section 2.1. Finally, owing to constraints of computing power, the production model is run at reduced depth (10 m) and time step (1 hour) resolution.

2.2.2. Extension to Case II

[20] As was stated in section 2.1.2, to give more accurate estimates of the in-water light field in optically complex case II waters an RTE such as HYDROLIGHT should be used. However, to use a coupled RTE-photosynthesis approach on satellite imagery (which typically comprises of several million pixels) is currently computationally restrictive. Therefore the HYDROLIGHT-photosynthesis coupled model has been reduced to a look-up table (PLUT) to speed up calculation. The PLUT construction process was split into three stages.

[21] First HYDROLIGHT, using 27 values of chlorophyll and 25 values of $a_{CDOM}(400\ nm)$ (see Table 1), was used to calculate the diffuse attenuation coefficient, $K_d(\lambda, Z)$ at 10 nm intervals between 400 and 700 nm and at depths of 0, 3, 5, 10 and 20 m. The code was run for noon on serial day 181 at 50°N, for a wind speed of 0 m s^{-1}, omitting the effects of bioluminescence, chlorophyll and CDOM fluorescence, and Raman scattering; the water was radiatively partitioned as in

Table 1. Basic Parameters, Which Act as Indices, Used to Generate the PLUT Together With Range and Increment

Entry	Range	Units	Increment	Number
Chl	0.01–9.0	mg m^{-3}	log increment	27
a_{CDOM}(400 nm)	0.01–6.0[a]	m^{-1}	log increment	25
Day length	2.0–24.0	hr	2 hours	12
iPAR	100–2900	μmol quanta m^{-2} s^{-1}	100	15
SST	5–25	°C	10	3
Total				364,500

[a]Additional "missing" CDOM entry added to LUT using equations (15) and (16).

section 2.1.2, and $a_{CDOM}(400)$ was converted into $a_{CDOM}(\lambda)$ using the equation

$$a_{CDOM}(\lambda) = 0.571 a_{CDOM}(400) \exp[-0.014(\lambda - 440)], \quad (14)$$

where $a_{CDOM}(400)$ is used rather than the more usual $a_{CDOM}(440)$ [*Sathyendranath et al.*, 2001] as it is a standard Moderate-Resolution Imaging Spectroradiometer (MODIS) product (absorp_coef_gelb [*Carder et al.*, 1999]). To allow the PLUT to be used on SeaWiFS imagery (where there is no standard a_{CDOM} product) and for a comparison run on the MODIS product suite, a "missing" a_{CDOM} LUT entry was instead created using the following equations:

$$a_{CDOM}(\lambda) = a_{CDOM}(440) \exp[-0.014(\lambda - 440)] \quad (15)$$

$$a_{CDOM}(440) = factor\left[a_w(440) + 0.06 A_{chl}(440)(Chl)^{0.65}\right], \quad (16)$$

following the equations of *Morel and Maritorena* [2001]. The leading factor in equation (16) was set to 0.8 [*Liu et al.*, 1999; *Smyth et al.*, 2002]. This is to account not only for the co-varying influence of autochthonous yellow substance but also pigmented non-photosynthetic particles. It was found, in preliminary runs of the model, that to produce realistic global PP totals the effects empirically described by equations (15) and (16) were required within the RTE rather than simply setting $a_{CDOM}(\lambda)$ to zero. This stage resulted in 675 tables of $K_d(\lambda, Z)$.

[22] Second, the atmospheric light field was modeled using 15 values of instantaneous PAR (iPAR) and 12 different values of day length (L) (Table 1). The iPAR is a standard MODIS product and is assumed to represent the maximum iPAR at noon allowing it to be converted to PAR(t) using the equation [*Kirk*, 2000]

$$PAR(t) = iPAR \sin(\pi t / L) \quad (17)$$

and converted to $E_d(\lambda, t)$ using the E_dLUT. The value of the average cosine for downwelling radiation, μ_0, was set to 0.86 [*Morel*, 1991]; this factor is important for the conversion from (in water) vector to scalar irradiance.

[23] Finally the *Morel* [1991] photosynthesis model was run using the outputs from the HYDROLIGHT and atmospheric modeling stages together with other required parameters shown in Table 2. As the values of $K_d(\lambda)$ were extracted from the HYDROLIGHT runs rather than the scalar irradiance (this was to keep the HYDROLIGHT modeling discrete from the atmospheric modeling as well as making the PLUT as general as possible) the following formula was used:

$$E_0(\lambda) = E_d(\lambda) \frac{1}{\mu_0} (1 + (0.425\mu_0 - 0.19) b/a)^{0.5}, \quad (18)$$

where a and b were taken from equations (8) and (10), respectively.

[24] The final 364,500 element, five-dimensional PLUT was then used to calculate primary production for five different scenarios shown in Table 3 with the day length for each pixel being calculated using the method of *Forsythe et al.* [1995].

3. Results

3.1. Model Validation

[25] Figure 1 shows a comparison between modeled and measured PP for 35 points from the EQPAC data set using the *Morel* [1991] photosynthesis model retaining the original *Morel* [1988] in-water light field. The model was run in single station mode with 1 m depth and 5 minute time resolution; the spectral values of irradiance were determined from daily integrated PAR using the E_dLUT. All of the modeled data points are within a factor of two of the measured values of PP. However, there is a tendency within this data set to underestimate values of PP when measured PP is greater than 600 mgC $m^{-2}d^{-1}$. The RMS error (in log space) is 0.16. This result is not surprising as the *Morel* [1991] model was parameterized in case I equatorial waters. When the PLUT was used to calculate PP (setting a_{CDOM} to "missing") and compared with the EQPAC data set the same RMS of 0.16 was obtained.

[26] Figure 2 shows a comparison between modeled and measured PP in the Irish Sea. The optical characteristics of

Table 2. Additional Parameters Required to Create the PLUT Together With Range and Increment

Parameter	Value(s)	Units	Increment	Description
Time step	...	minutes	5	model time step
Wavelength	400–700	nm	5	wavelength interval
Depth	0–300	m	1	model depth interval
Euphotic depth	1%	m	...	depth to which production calculated
β	0.01	...	...	photoinhibition parameter[a]
KPUR(20°C)	80	μmol quanta $m^{-2}s^{-1}$	-	light/physiological parameter[b]

[a]Using equation (5).
[b]Using equation (3).

Table 3. Data Scenarios Using the PLUT

Scenario Name	Sensor	Date Range	SST Product	CDOM Product	Chl Product
SeaWiFS	SeaWiFS	1998–2003	Pathfinder	"missing"[a]	OC4V4[b]
MODIS a2	MODIS	2000–2003[c]	MODIS SST	"missing"[a]	MODIS chlor_a_2
MODIS a2+CDOM	MODIS	2000–2003[c]	MODIS SST	MODIS[d]	MODIS chlor_a_2
MODIS a3	MODIS	2000–2003[c]	MODIS SST	"missing"[a]	MODIS chlor_a_3
MODIS a3+CDOM	MODIS	2000–2003[c]	MODIS SST	MODIS[d]	MODIS chlor_a_3

[a]Value $a_{CDOM}(\lambda)$ calculated using equations (15) and (16).
[b]*O'Reilly et al.* [1998].
[c]Data starting March 2000.
[d]Denotes absorp_coef_gelb [*Carder et al.*, 1999].

the Irish Sea are mixed case I and case II [*Tilstone et al.*, 2004] with contributions from CDOM and SPM, as well as chlorophyll, to the IOPs. The left panel uses the *Morel* [1991] model retaining the original *Morel* [1988] light field and shows that PP is overestimated by as much as a factor of 10 in some cases. However, when the effects of CDOM and SPM are included and the photosynthesis model of *Morel* [1991] coupled with HYDROLIGHT (right panel), the estimates of production are improved. The slope of the log regression changes from 0.36 to 0.95 and the RMS is improved from 0.48 to 0.23 (in log space). The Irish Sea study [*Tilstone et al.*, 2004], from which these data are taken, found that CDOM had a more significant effect on estimates of PP than SPM and on the basis of these results it was decided to construct the PLUT using values of CDOM and chlorophyll and to assume that the effect of SPM on PP was comparatively small.

3.2. Global Estimates of PP

[27] The first two columns of Table 4 show the yearly global PP totals using SeaWiFS data as input to the *Morel* [1991] model retaining the *Morel* [1988] in-water light field, which propagates light through the water column using equation (7), and the PLUT which uses values of $K_d(\lambda)$ using HYDROLIGHT. The PLUT values are for the "missing" CDOM entries of the look-up table and have used equation (16) to determine the autochthonous CDOM and non-photosynthetic pigment absorption. Another important thing to note is that the *Morel* [1988] formulation uses the pure water absorption coefficients of *Smith and Baker* [1981] and the PLUT those of *Pope and Fry* [1997]. The PLUT gives a reduction in the global estimates of PP by around 7% to a 52.8 Gt C yr^{-1} average for the SeaWiFS mission period.

[28] The remainder of Table 4 shows a comparison between the yearly global PP totals using the scenarios shown in Table 3. MODIS data for 2000 is restricted to March–December only and shown here to give relative differences between the MODIS data combinations. When the MODIS CDOM product (absorp_coef_gelb) is used, with both the MODIS chlorophyll algorithms, there is a reduction in the amount of global PP by around 2 Gt C yr^{-1} (4%). Overall the MODIS chlor_a_3 algorithm gives the highest values of production (54.9 Gt C yr^{-1}) and the MODIS chlor_a_2 combined with CDOM the lowest (51.6 Gt C yr^{-1}). As was expected the SeaWiFS global PP totals were close to those obtained by MODIS chlor_a_2, the SeaWiFS analogue algorithm.

[29] Figures 3 and 4 show the ocean basin breakdown by month averaged over the entire SeaWiFS (1998–2003) and MODIS (2000–2003) missions, respectively. All sensors and approaches give similar results for the various basins. The global ocean basin gives between 4 and 5 Gt C $month^{-1}$ with little in the way of a seasonal cycle. Both the Southern and Arctic oceans have a marked seasonality. The effect of CDOM in these high latitude seas is minimal; however, it is noticeable that the MODIS chlor_a_3 algorithm gives 50% higher production in the austral summer when compared with the MODIS chlor_a_2 (not shown) and SeaWiFS formulations in the Southern Ocean. The Pacific Ocean has two peaks in PP in May and August, this being more marked in the MODIS chlor_a_3 formulation. The early bloom is due to the Northern Hemisphere spring bloom and the latter is due to an equatorial blooming. Interestingly, putting the CDOM product into the PP calculations causes a marginal increase in the value of production

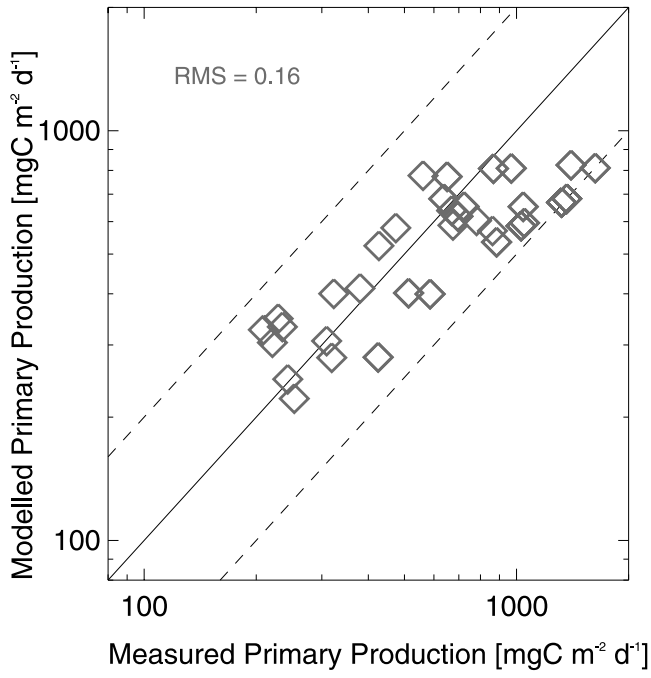

Figure 1. Modeled versus measured values of PP using the predominantly case I EqPac data set. The modeled PP uses the *Morel* [1991] PP model retaining the *Morel* [1988] in-water light field and is run in single station mode. This comparison was carried out as part of the PPARR3 experiment [*Carr et al.*, 2005] and also forms part of the work by *Friedrichs et al.* [2003]. See color version of this figure in the HTML.

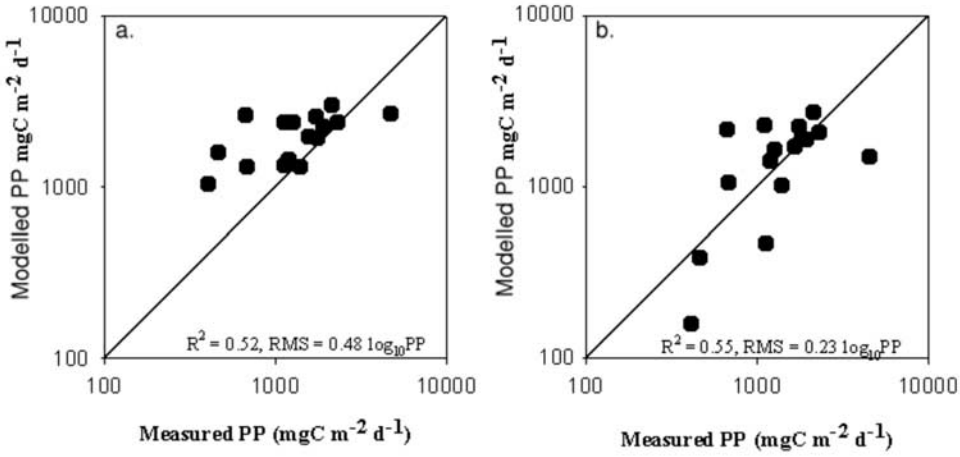

Figure 2. Modeled versus measured values of PP for the predominantly case II Irish Sea. (a) The *Morel* [1991] model retaining the *Morel* [1988] in-water light field; (b) effect of the inclusion of CDOM and SPM within the coupled photosynthesis radiative transfer model.

in the Pacific. This is due to the calculation for "missing" CDOM (i.e., equation (16)) overestimating the absorption compared with that derived from the satellite data in the ultra-oligotrophic regions of the sub-tropical Pacific. The Atlantic peak in PP is a more gradual phenomenon with the highest PP being between May and September and therefore heavily biased toward the Northern Hemisphere summer. The Atlantic also shows the greatest effect of CDOM; there is around a 10% reduction in PP in the summer months for both chlor_a_2 and chlor_a_3 formulations. That the effect of CDOM is greater in the boreal summer is a slightly surprising result as riverine discharge, and hence CDOM input, would be at its maximum in the winter months. This result could be partly due to the constraints of ocean color determination during the winter (viewing geometry) and also increased cloudiness during these months. The Indian Ocean shows a slight peak in production in the months following the summer monsoon.

[30] Figure 5 shows the relative basin contributions to the global PP totals. The greatest differences are between chlorophyll algorithms rather than the addition or omission of the CDOM field. The use of the chlor_a_3 data set, rather than either chlor_a_2 or SeaWiFS as the input chlorophyll field, yields around a 3% increase to the value of PP in the Southern Ocean. It seems from Figure 5 that correcting the irradiance profile to account for case II waters has a negligible global and basin scale impact. This could be due to several mitigating factors such as that the global ocean is predominantly case I and that the "missing" CDOM formulations are adequately describing the non-photosynthetic absorption component in the majority of case I and II areas. It could be that at the sub 18 km scale the effect of CDOM, and hence implementation of the PLUT, proves to be important: This is very hard to substantiate however without adequate in situ validation.

4. Discussion

[31] It was found in the Irish Sea that the effect of CDOM upon the calculated PP values was far greater than that of SPM; this influenced the decision to omit the effect of SPM in the production look-up table. This result could partly be due to the way that the IOPs are parameterized within HYDROLIGHT and subsequently used in the photosynthesis model. First the IOP formulation only allows detrital matter associated with phytoplankton and the SPM itself to contribute to the scattering; there is no $a_{SPM}(\lambda)$ term. To properly account for any $a_{SPM}(\lambda)$ term globally would be an extremely difficult proposition given the wide variation in mineralogy worldwide. Second, the physical effect of only allowing SPM to scatter is to redistribute the angular light field within the water column, turning vector ($E_d(\lambda)$) into scalar ($E_0(\lambda)$) irradiance. As phytoplankton is not predisposed to receiving light from any particular direction the effect of adding SPM to the water column has little effect. This may be common for other coastal regions where SPM does not exceed 5 mg m^{-3} but in regions of high SPM, such as estuaries, this assumption may not hold. *Joint and Pomroy* [1980] found that turbidity in the Bristol Channel reduced PP; in addition, *Babin et al.* [2003] and *Ferrari et al.* [2003] have shown that SPM also represents significant absorption either through colored absorbing (Fe) minerals or through highly absorbing organic material. The Irish Sea is representative of other European regions such as the Loire and Seine plumes [*Ferrari et al.*, 2003]; however, the omission of SPM from the PLUT may impact on retrievals of PP in areas like the Rhine [*Ferrari et al.*, 2003], Schelde,

Table 4. Comparison Between Annual Global Estimates of PP Using the Original Model and the Various Scenarios Described in Table 3 Using the PLUT[a]

Year	Original	SeaWiFS	MODIS a2	MODIS a2+CDOM	MODIS a3	MODIS a3+CDOM
1998	55.9	51.7	...	...	...	...
1999	57.5	53.4	...	...	...	...
2000	57.5	53.9	47.7[b]	46.2[b]	49.4[b]	48.6[b]
2001	57.0	52.9	54.0	51.6	54.9	53.0
2002	56.7	52.5	53.0	51.7	54.6	53.9
2003	56.7	52.5	53.9	51.7	55.0	53.3

[a]Original model is that of *Morel* [1991] retaining the *Morel* [1988] in-water light field.
[b]Data starting March 2000.

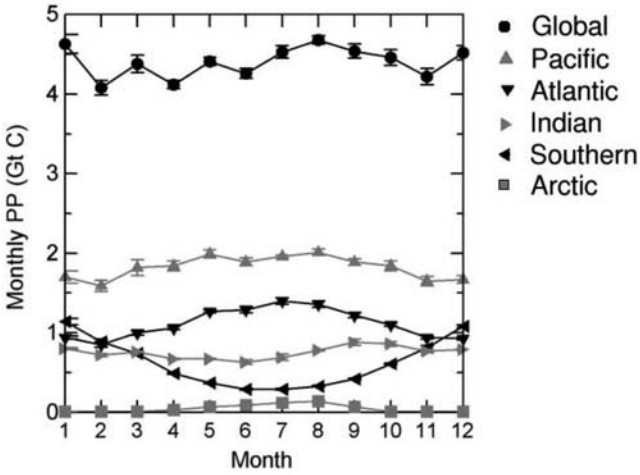

Figure 3. Average PP per month calculated using the PLUT over the various ocean basins using SeaWiFS data (1998–2003). Error bars are the standard deviation from the mean plotted.

Mississippi [*Miller and McKee*, 2004], and even bigger estuarine systems such as the Nile, Ganges, Congo and Amazon. On the global scale (18 km pixels) though these seemingly large local, perhaps regional, effects on the PP may be offset by the fact that they are generally restricted to the coastal zone.

[32] This paper has also assumed vertically invariant profiles of chlorophyll which undoubtedly introduces some error to the PP estimates [*Morel and Berthon*, 1989; *Antoine and Morel*, 1996]. However, *Behrenfeld and Falkowski* [1997a] found that including the vertical structure of chlorophyll did not statistically improve the predictive capacity of their model. Additionally, for consistency, if vertical variability in chlorophyll is introduced then it must also be introduced for CDOM. This is fraught with difficulty as other factors, such as photo-oxidation, must be considered leading to a considerable increase in model complexity.

[33] The similar but unrelated papers of *Liu et al.* [1999] and *Smyth et al.* [2002] give a leading factor in the $a_{CDOM}(\lambda)$ formulation of 0.8 rather than the previous published values of 0.2 [*Morel*, 1991; *Morel and Maritorena*, 2001]. This factor happens to be important when used in conjunction with the pure water absorption values of *Pope and Fry* [1997] compared with the earlier values of *Smith and Baker* [1981]. This is shown in Figure 6: The figure is composed of equation (16) using the *Pope and Fry* [1997] $a_w(\lambda)$ values and a leading factor of 0.8 (PF); the *Smith and Baker* [1981] values (crosses) are calculated using equations (20a) and (20b) from *Morel* [1991] and a leading factor of 0.2 (SB). For low values of chlorophyll the SB formulation gives lower values of spectral absorption than

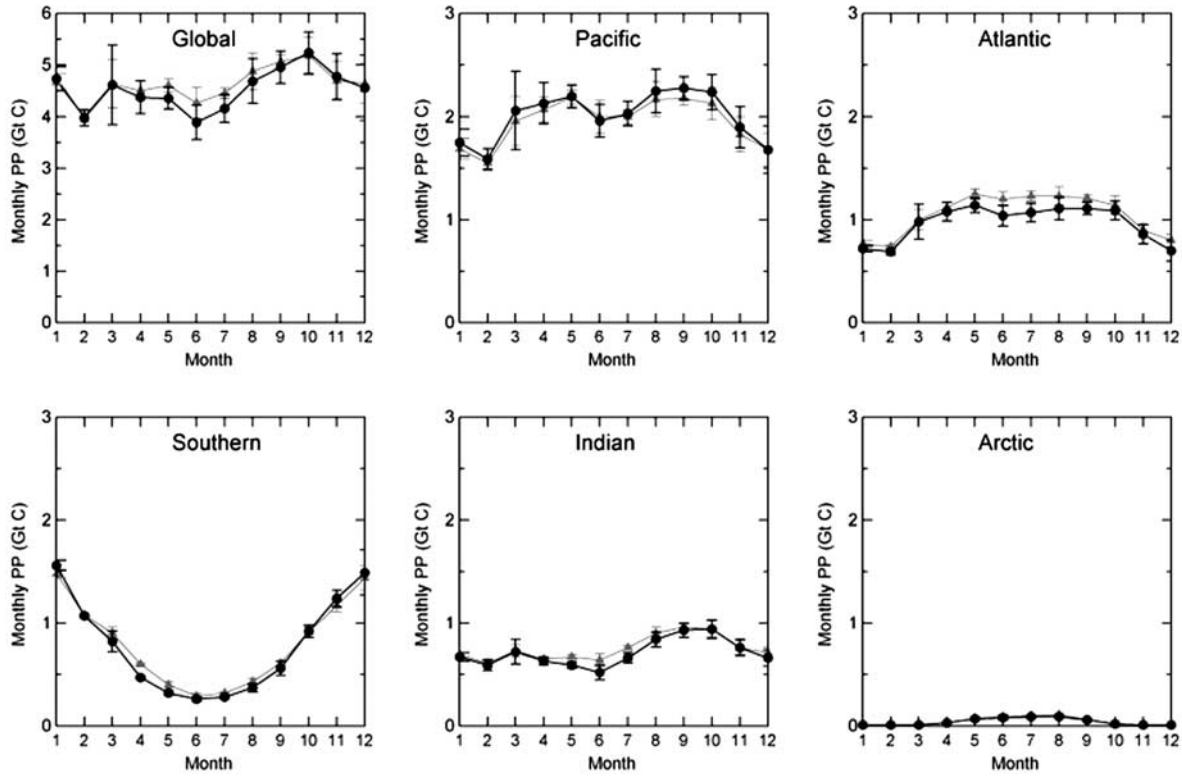

Figure 4. Average PP per month calculated using the PLUT over the various ocean basins using MODIS chlor_a_3 algorithm with (black) and "missing" (shaded) CDOM.

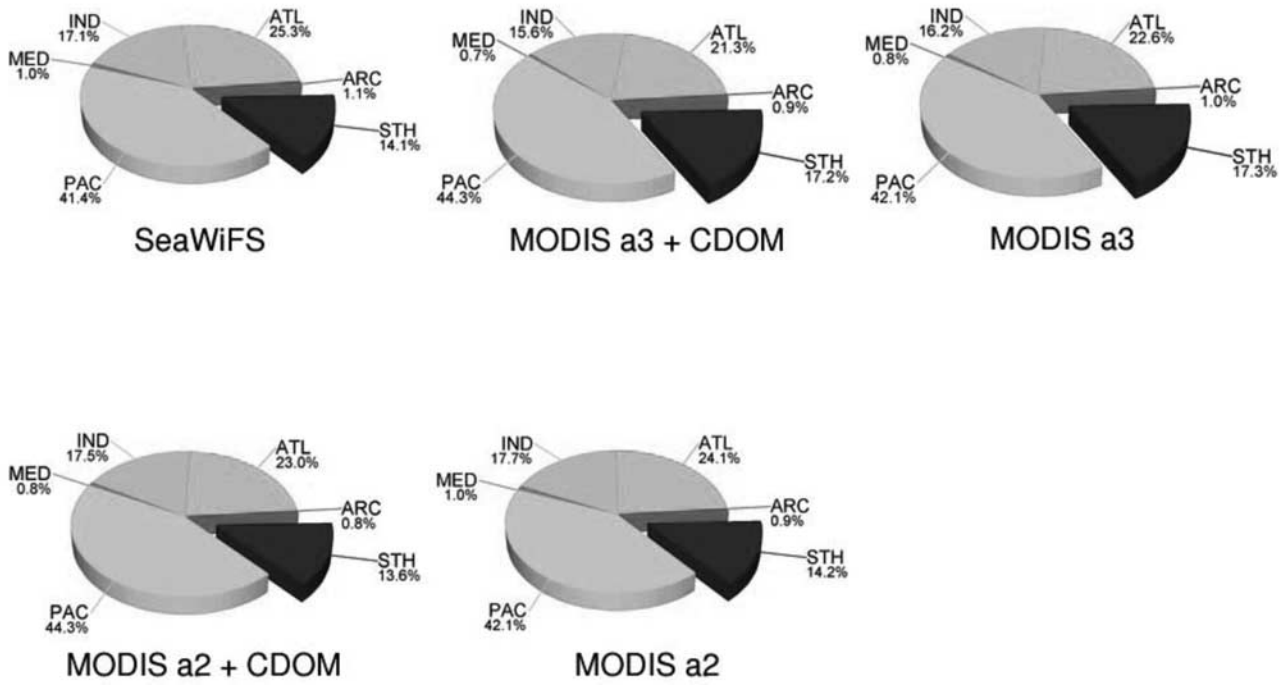

Figure 5. Basin contributions to the overall global total PP, calculated using the PLUT, for the various data scenarios shown in Table 3. See color version of this figure in the HTML.

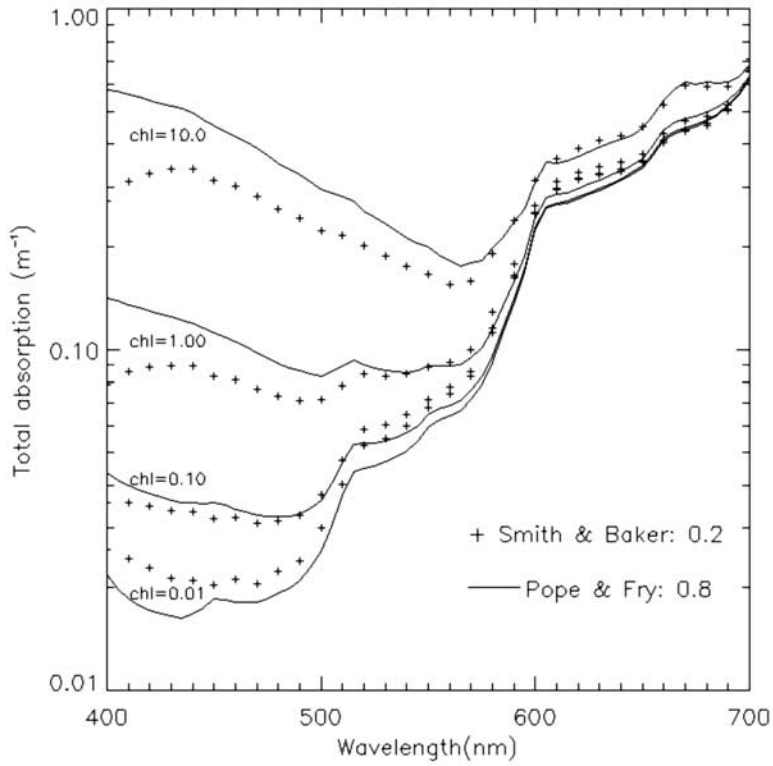

Figure 6. Total absorption as a function of wavelength and chlorophyll concentration (mg m^{-3}) using work by *Pope and Fry* [1997] with a leading factor of 0.8 in equation (16) (solid line) and *Smith and Baker* [1981] with a leading factor of 0.2 in equations (20a) and (20b) of *Morel* [1991] (plus signs).

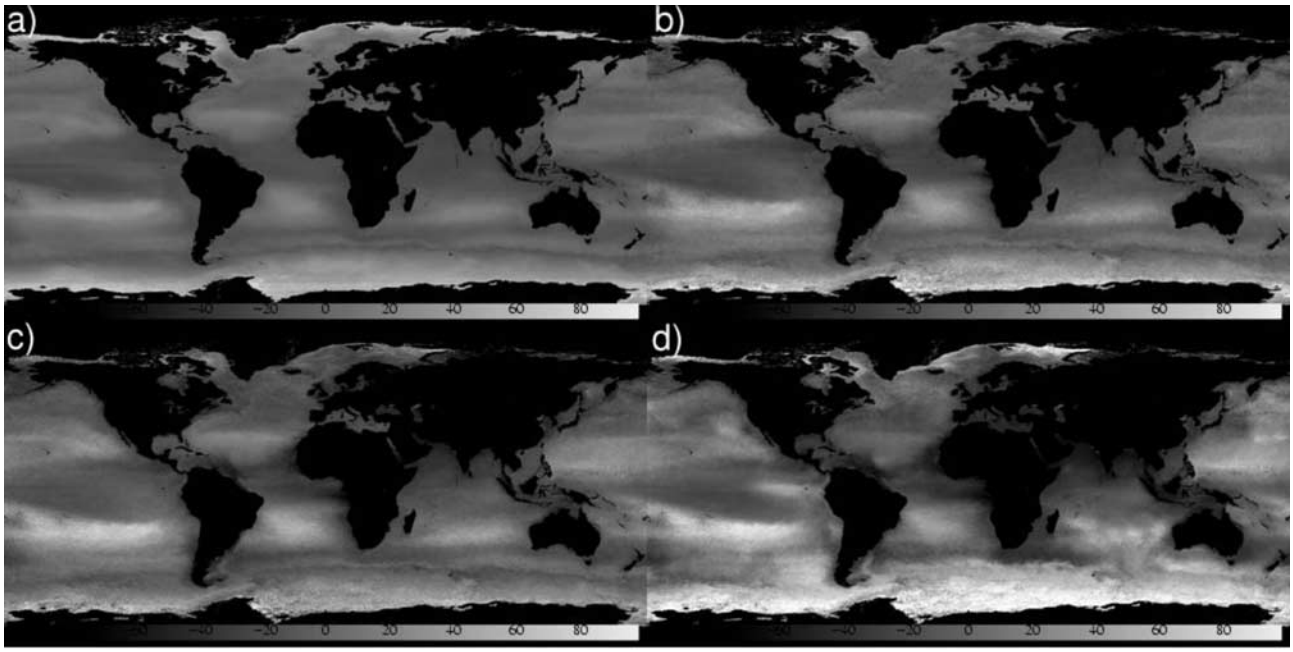

Figure 7. Percentage differences between the *Morel* [1991], retaining the original *Morel* [1988] in-water light field, modeled global estimates of PP using SeaWiFS chlorophyll as input and (a) PLUT using SeaWiFS chlorophyll as input, (b) PLUT using MODIS chlor_a_2 as input and "missing" CDOM, (c) PLUT using MODIS chlor_a_2 and absorp_coef_gelb, and (d) PLUT using MODIS chlor_a_3 and absorp_coef_gelb.

the PF formulation in the photosynthetically important 400–550 nm range. This situation is reversed, however, when chlorophyll values are around 0.1 mg m^{-3}. Interestingly, the global averaged chlorophyll, determined from SeaWiFS, is around 0.22 mg m^{-3}. From Figure 6 alone it can be inferred that the global totals of PP using the PLUT will be lower than those determined by the *Morel* [1991] model using the *Morel* [1988] in-water light field. When the leading factor of 0.2 was used with $a_w(\lambda)$ of *Pope and Fry* [1997] the global totals of production for the "missing" CDOM case rose to around 70 Gt C yr^{-1}, a value far in excess of the current estimations of global annual PP.

[34] Figure 6 explains some of the regional differences between the various scenarios: These are shown in Figure 7. Taking Figure 7 as a whole could lead to the conclusion that the effect of the satellite determined CDOM field is small and can be better parameterized on the global scale using equation (16) and a leading factor of 0.8. However, if accurate estimates of PP are required in optically complex case II waters, and possibly in upwelling regions, then it is important to retain the CDOM retrieved values as an input. Figure 7a shows the difference between the *Morel* [1991] model retaining the *Morel* [1988] in-water light field and the PLUT setting CDOM to "missing," i.e., using equation (16); both use SeaWiFS chlorophyll as input. The low chlorophyll regions of the globe, such as the ultra-oligotrophic southern Pacific, show an increase in the value of mean annual production by around 50% when the PLUT is used. An increase in production is also seen in the High Nitrate Low Chlorophyll regions of the Southern Ocean by around 60%. The case II regions of the globe, such as the North Sea, there is a slight reduction in PP, of around 10%. The largest reductions are in the equatorial upwelling regions and the northern Indian ocean. This is due to a combination of the different IOP formulation and the use of a radiative transfer approach. Figure 7b shows the difference between the *Morel* [1991] model using the *Morel* [1988] in-water light field on SeaWiFS chlorophyll data and the PLUT (setting CDOM to "missing") this time using MODIS chlor_a_2 as the input. The basic regional patterns are the same but the increase in PP compared with Figure 7a are solely due to the differences between the SeaWiFS and MODIS sensors, since the MODIS chlor_a_2 algorithm is the SeaWiFS analogue equation. These changes are again more pronounced in the sub-tropical oceanic gyres and the circumpolar Southern Ocean. Figures 7c and 7d show how the addition of the CDOM (absorp_coeff_gelb) product has upon the estimates of production for the MODIS chlor_a_2 and chlor_a_3 inputs respectively. Both Figures 7c and 7d give increases of production in the southern Pacific gyre. This is due to the overestimation of CDOM by equation (16) in this region. However, there is a reduction of PP in major upwelling regions, such as the Benguela, off west Africa, and in case II waters such as the North Sea, by around 30–40%. Figure 7d shows greatly enhanced (by a factor of 2) production in the Southern Ocean due to the higher estimates of chlorophyll by the chlor_a_3 algorithm. Accurate retrievals of chlorophyll in the Southern Ocean, however, are still a contentious issue. *Moore and Abbott* [2000] found SeaWiFS to give good agreement with in situ measurements whereas estimates presented by *Arrigo et al.* [1994] show SeaWiFS to underestimate chlorophyll by around 40%.

[35] These findings raise the issue of accuracy of the MODIS chlorophyll and CDOM algorithms. *Blondeau-Patissier et al.* [2004] found that the chlor_a_3 algorithm was the most accurate of the MODIS chlorophyll algorithms but that the absorp_coeff_gelb product consistently overestimated a_{CDOM} in European coastal waters; this implies that PP would be consistently underestimated in these regions. In the Baltic, *Darecki and Stramski* [2004] found that chlorophyll was consistently overestimated using MODIS chlor_a_2 and chlor_a_3 and that a_{CDOM} was consistently underestimated; this implies that PP would be consistently overestimated in the Baltic. Both these studies highlight that the satellite PP estimates in coastal regions may not be entirely accurate, however satellite still represents the only means of retrieving global PP at high temporal and spatial resolution.

5. Conclusions

[36] A primary production look-up table (PLUT) has been constructed to use as inputs global fields of chlorophyll, CDOM, PAR and SST derived from satellite data. The PLUT uses the photosynthesis model of *Morel* [1991] coupled with the radiative transfer equation code HYDROLIGHT [*Mobley*, 1995]. The advantages of using the PLUT are that it (1) speeds up calculation of global PP by two orders of magnitude (which incidentally allows it to be used for the near-real time calculation of PP); (2) includes a more accurate formulation for propagating light through the water column [*Liu et al.*, 1999] and (3) allows the inclusion of CDOM via the IOP calculations. The global totals of PP using the PLUT vary between 51.7 Gt C yr^{-1} and 55 Gt C yr^{-1} depending upon the sensor and data input scenario used. It would seem from this that the effect of using CDOM in the RTE is small on the basin and global scale. However, on the local and regional scales this paper has shown the effect of CDOM to be important for optically complex case II waters. This paper has also shown that it is important for the "missing" CDOM case to use a leading factor in equation (16) of 0.8 when used in conjunction with the pure water absorption values of *Pope and Fry* [1997]. The most consistent set of data to use when determining global PP totals would seem to be the MODIS chlor_a_3 together with the CDOM absorp_coef_gelb as input to the PLUT as both of these are derived using the *Carder et al.* [1999] algorithms.

[37] **Acknowledgments.** This work has been carried out as part of the EU PROOF (EUK3-1999-00103) project and NERC Marine Productivity thematic (Grant No. GST/02/2765) and is CASIX contribution 35. The MODIS and SeaWiFS data were obtained from the Goddard DAAC and use of these data are in accordance with the SeaWiFS Research Data Use Terms and Conditions Agreement. The authors are indebted to John Beisley for his computer coding skills and to Curt Mobley for making the HYDROLIGHT code available to us. Figure 1 was produced by Marjy Friedrichs as part of the NASA PPARR3 experiment.

References

Antoine, D., and A. Morel (1996), Oceanic primary production: 1. Adaption of spectral light-photosynthesis model in view of application to satellite chlorophyll observations, *Global Biogeochem. Cycles*, *10*, 43–55.

Antoine, D., J. M. Andre, and A. Morel (1996), Oceanic primary production: 2. Estimation at global scale from satellite (Coastal Zone Color Scanner) chlorophyll, *Global Biogeochem. Cycles*, *10*, 57–69.

Arrigo, K. R., C. R. McClain, J. K. Firestone, C. W. Sullivan, and J. C. Comiso (1994), A comparison of CZCS and in situ pigment concentrations in the Southern Ocean, *NASA Tech. Memo., 104566*, 30–34.

Babin, M., D. Stramski, G. M. Ferrari, H. Claustre, A. Bricaud, G. Obolensky, and N. Hoepffner (2003), Variations in the light absorption coefficients of phytoplankton, nonalgal particles, and dissolved organic matter in coastal waters around Europe, *J. Geophys. Res.*, *108*(C7), 3211, doi:10.1029/2001JC000882.

Behrenfeld, M. J., and P. G. Falkowski (1997a), Photosynthetic rates derived from satellite-based chlorophyll concentration, *Limnol. Oceanogr.*, *42*, 1–20.

Behrenfeld, M. J., and P. G. Falkowski (1997b), A consumer's guide to phytoplankton primary productivity models, *Limnol. Oceanogr.*, *42*, 1479–1491.

Blondeau-Patissier, D., G. H. Tilstone, V. Martinez-Vicente, and G. F. Moore (2004), Comparison of bio-physical marine products from SeaWiFS MODIS and a bio-optical model with in situ measurements from northern European waters, *J. Opt. A Pure Appl. Opt.*, *6*, 875–889.

Campbell, J., et al. (2002), Comparison of algorithms for estimating primary productivity from surface chlorophyll, temperature, and irradiance, *Global Biogeochem. Cycles*, *16*(3), 1035, doi:10.1029/2001GB001444.

Carder, K. L., F. R. Chen, Z. P. Lee, and S. K. Hawes (1999), Semianalytic Moderate Resolution Imaging Spectrometer algorithms for chlorophyll *a* and absorption with bio-optical domains based on nitrate-depletion temperatures, *J. Geophys. Res.*, *104*, 5403–5421.

Carr, M.-E., et al. (2005), A comparison of global estimates of marine primary production from ocean color, *Deep Sea Res., Part II*, in press.

Darecki, M., and D. Stramski (2004), An evaluation of MODIS and SeaWiFS bio-optical algorithms in the Baltic Sea, *Remote Sens. Environ.*, *89*, 326–350.

Doerffer, R. (2002), Protocols for the validation of MERIS water products, *Tech. Rep. PO-TN-MEL-GS-0043*, Eur. Space Agency, Paris.

Ferrari, G. M., F. G. Bo, and M. Babin (2003), Geo-chemical and optical characterizations of suspended matter in European coastal waters, *Estuarine Coastal Shelf Sci.*, *57*, 17–24.

Field, C. B., M. J. Behrenfeld, J. T. Randerson, and P. Falkowski (1998), Primary production of the biosphere: Integrating terrestrial and oceanic components, *Science*, *281*, 237–240.

Forsythe, W. C., E. J. Rykiel, R. S. Stahl, H. Wu, and R. M. Schoolfield (1995), A model comparison for daylength as a function of latitude and day of year, *Ecol. Modell.*, *80*, 87–95.

Friedrichs, M., M.-E. Carr, R. Barber, and M. Schmeltz (2003), Comparison of primary production estimates in the tropical Pacific Ocean, *Eos Trans. AGU*, *84*(52), Ocean Sci. Meet. Suppl., Abstract OS22A-04.

Frouin, R., and R. T. Pinker (1995), Estimating photosynthetically active radiation (PAR) at the Earth's surface from satellite observations, *Remote Sens. Environ.*, *51*, 98–107.

Gregg, W. W., and K. L. Carder (1990), A simple spectral solar irradiance model for cloudless maritime atmospheres, *Limnol. Oceanogr.*, *35*, 1657–1675.

Joint, I. R., and A. J. Pomroy (1980), Primary production in a turbid estuary, *Estuarine Coastal Shelf Sci.*, *13*, 303–316.

Joint, I. R., and A. J. Pomroy (1986), Photosynthetic characteristics of nanoplankton and picoplankton from the surface mixed layer, *Mar. Biol.*, *92*, 465–474.

Kirk, J. T. O. (2000), *Light and Photosynthesis in Aquatic Ecosystems*, 2nd ed., Cambridge Univ. Press, New York.

Kolber, Z. S., and P. G. Falkowski (1993), Use of active fluorescence to estimate phytoplankton photosynthesis in-situ, *Limnol. Oceanogr.*, *38*, 1646–1665.

Liu, C. C., J. D. Woods, and C. D. Mobley (1999), Optical model for use in oceanic ecosystem models, *Appl. Opt.*, *38*, 4475–4485.

McClain, E. P., W. G. Pichel, and C. C. Walton (1985), Comparative performance of AVHRR-based multichannel sea surface temperature, *J. Geophys. Res.*, *90*, 11,587–11,601.

Miller, R. L., and B. A. McKee (2004), Using MODIS Terra 250 m imagery to map concentrations of total suspended matter in coastal waters, *Remote Sens. Environ.*, *93*, 259–266.

Mobley, C. D. (1994), *Light and Water: Radiative Transfer in Natural Waters*, Elsevier, New York.

Mobley, C. D. (1995), *HYDROLIGHT 3.0 User's Guide*, SRI Int., Menlo Park, Calif.

Moore, J. K., and M. R. Abbott (2000), Phytoplankton chlorophyll distributions and primary production in the Southern Ocean, *J. Geophys. Res.*, *105*, 28,709–28,722.

Morel, A. (1974), Optical properties of pure seawater, in *Optical Aspects of Oceanography*, edited by N. G. Jerlov and E. S. Nielsen, pp. 1–24, Elsevier, New York.

Morel, A. (1988), Optical modelling of the upper ocean in relation to its biogenous matter content (Case I waters), *J. Geophys. Res.*, *93*, 10,749–10,768.

Morel, A. (1991), Light and marine photosynthesis: A spectral model with geochemical and climatological implications, *Prog. Oceanogr.*, *26*, 263–306.

Morel, A., and J. F. Berthon (1989), Surface pigments, algal biomass profiles, and potential production of the euphotic layer: Relationships reinvestigated in view of remote-sensing applications, *Limnol. Oceanogr.*, *34*, 1545–1562.

Morel, A., and S. Maritorena (2001), Bio-optical properties of oceanic waters: A reappraisal, *J. Geophys. Res.*, *106*, 7163–7180.

Morel, A., D. Antoine, M. Babin, and Y. Dandonneau (1996), Measured and modeled primary production in the northeast Atlantic (EUMELI JGOFS program): The impact of natural variations in photosynthetic parameters on model predictive skill, *Deep Sea Res., Part I*, *43*, 1273–1304.

O'Reilly, J. E., S. Maritorena, B. G. Mitchell, D. A. Siegel, K. L. Carder, S. A. Garver, M. Kahru, and C. McClain (1998), Ocean color chlorophyll algorithms for SeaWiFS, *J. Geophys. Res.*, *103*, 24,937–24,953.

Petzold, T. J. (1972), Volume scattering functions for selected natural waters, *Tech. Rep. 71-78*, Scripps Inst. of Oceanogr., Visibility Lab., San Diego, Calif.

Platt, T., and S. Sathyendranath (1991), Biological production models as elements of coupled, atmosphere-ocean models for climate research, *J. Geophys. Res.*, *96*, 2585–2592.

Platt, T., C. L. Gallegos, and W. G. Harrison (1980), Photoinhibition of photosynthesis in natural assemblages of marine phytoplankton, *J. Mar. Res.*, *38*, 687–701.

Pope, R. M., and E. S. Fry (1997), Absorption spectrum (380–700 nm) of pure water: II. Integrating cavity measurements, *Appl. Opt.*, *36*, 8710–8722.

Prieur, L., and S. Sathyendranath (1981), An optical classification of coastal and oceanic waters based on the specific spectral absorption curves of phytoplankton pigments, dissolved organic matter, and other particulate materials, *Limnol. Oceanogr.*, *26*, 671–689.

Reed, R. K. (1977), On estimating insolation over the ocean, *J. Phys. Oceanogr.*, *7*, 482–485.

Sathyendranath, S., G. Cota, V. Stuart, H. Maass, and T. Platt (2001), Remote sensing of phytoplankton pigments: A comparison of empirical and theoretical approaches, *Int. J. Remote Sens.*, *22*, 249–273.

Smith, R. C., and K. S. Baker (1981), Optical properties of the clearest natural waters (200–800 nm), *Appl. Opt.*, *20*, 177–184.

Smyth, T. J., G. F. Moore, S. B. Groom, P. E. Land, and T. Tyrrell (2002), Optical modeling and measurements of a coccolithophore bloom, *Appl. Opt.*, *41*, 7679–7688.

Tilstone, G. H., T. J. Smyth, V. Martinez-Vicente, and S. B. Groom (2004), Inherent optical properties of the Irish Sea and their effect on primary production algorithms for remote sensing, in *Ocean Optics XVII* [CD-ROM], Off. of Naval Res., Washington, D. C.

Williams, P. J. L. B., R. C. T. Raine, and J. R. Bryan (1979), Agreement between the ^{14}C and oxygen methods of measuring phytoplankton production: Reassessment of the photosynthetic quotient, *Oceanol. Acta*, *2*, 411–416.

Wollast, R. (1998), Evaluation and comparison of the global carbon cycle in the coastal zone and in the open ocean, in *The Sea*, vol. 10, *The Global Coastal Ocean: Processes and Methods (Ideas and Observations on the Progress of the Studies of the Seas)*, edited by K. H. Brink and A. R. Robinson, pp. 213–252, John Wiley, New York, Hoboken, N. J.

S. B. Groom, T. J. Smyth, and G. H. Tilstone, Plymouth Marine Laboratory, Prospect Place, Plymouth, Devon, UK, PL1 3DH. (tjsm@pml.ac.uk)